






Hierarchical Microenergy Hub Sizing and Placement in Integrated Electricity and Natural Gas Distribution Systems

Seyed Abbas Seifossadat , Mohammad Rastegar , *Member, IEEE*, Mohammad Mohammadi , *Member, IEEE*, Soroush Senemmar , *Student Member, IEEE*, and Jie Zhang , *Senior Member, IEEE*

Abstract—The integration of different energy carriers is a key factor to improve the energy network performance. A micro-energy hub (μ EH) concept has recently been proposed in the integrated electricity and natural gas distribution systems (IENGDSs), for generating, converting, storing, and managing different types of energy at the customer level. To improve the performance of μ EH, this paper proposes a hierarchical optimization-based model to optimize the sizes of μ EH components and locations of μ EHs in the IENGDS. The operation and structural sizing constraints of the μ EHs are first determined. Then the optimal electricity network buses and natural gas nodes for installing μ EHs are determined, considering the operational constraints of IENGDS. The objective in both steps is to minimize operation and investment costs. Moreover, the impacts of seasonal climate changes on energy demands and prices are considered during the planning horizon. Furthermore, the uncertainties in demands and renewable energy generation are quantified with a two-stage stochastic programming framework. The effectiveness of the proposed method is evaluated on an IENGDS that consists of an IEEE 33-bus distribution system and a Belgian 20-node natural gas system. Numerical simulations demonstrate that the optimal hierarchical planning model can improve total line losses and reduce the total purchased electricity from the upstream network and total imported natural gas from gas wells. The simulation results show that if the hierarchical optimization process is not performed in determining optimal placement of μ EHs, then IENGDS may operate with electricity network congestion or natural gas pressure violations during the planning horizon.

Index Terms—Integrated electricity and natural gas distribution systems (IENGDSs), microenergy hub, planning, stochastic programming.

NOMENCLATURE

Indices

y Index of years

Manuscript received 1 May 2021; revised 29 July 2021 and 2 November 2021; accepted 6 December 2021. Date of publication 20 January 2022; date of current version 9 December 2022. (*Corresponding author: Mohammad Mohammadi.*)

Seyed Abbas Seifossadat, Mohammad Rastegar, and Mohammad Mohammadi are with the Department of Power and Control, School of Electrical and Computer Engineering, Shiraz University, Shiraz 71557-13876, Iran (e-mail: a.seifossadat@shirazu.ac.ir; m.mohammadi@shirazu.ac.ir; m_mohammadi@shirazu.ac.ir).

Soroush Senemmar is with the Department of Electrical and Computer Engineering, The University of Texas at Dallas, Richardson, TX 75080 USA (e-mail: soroush.senemmar@utdallas.edu).

Jie Zhang is with the Department of Mechanical Engineering, The University of Texas at Dallas, Richardson, TX 75080 USA (e-mail: jiezhang@utdallas.edu).

Digital Object Identifier 10.1109/JSYST.2021.3136586

s Index of seasons
 t Index of time
 c, e Index of μ EH
 i, j Index of electricity network buses
 g, n, m Index of natural gas nodes
 $w(n)$ Index of gas wells in natural gas systems
 sc Index of scenarios
 Ω_B Set of electricity network buses
 Ω_N Set of natural gas nodes
 Ω_G Set of gas wells
 μEH Set of μ EHs

Parameters

ND_s Number of days in each season
 $C_{y,s,t}^{\mu EH \text{ electricity}}$ Electricity tariff for μ EH operator
 $C_{y,s,t}^{\mu EH \text{ gas}}$ Natural gas tariff for μ EH operator
 $C_{y,s}^{\text{Boiler/CHP/ESS/PV}}$ Investment cost of gas boiler, CHP, ESS, and PV panel
 $\eta_{y,s,t,c,sc}^{ge \text{ CHP}}$ G2P conversion efficiency of CHP at μ EH c
 $\beta_{y,s,t,c,sc}^{ph \text{ CHP}}$ P2H ratio of CHP at μ EH c
 η_c^{Boiler} Efficiency of gas boiler
 $H_{y,s,t,c,sc}^{\text{Load}_{\mu EH}}$ Heat demand at μ EH c
 $P_{y,s,t,c,sc}^{\text{Load}_{\mu EH}}$ Electricity demand at μ EH c
 η^{ch}, η^{dch} Charging and discharging efficiency of ESS
 P_{sh}^{Max} Maximum charging rate of ESS
 P_{dch}^{Max} Maximum discharging rate of ESS
 $P_{s,t,sc}^{\text{PV}_{base}}$ Standard energy output from a 1-kW PV panel
 $P_{\text{Input}_{\mu EH}}^{\text{Max}}$ Maximum input electricity of μ EH c
 $C_{\text{Input}_{\mu EH}}^{\text{Max}}$ Maximum input natural gas of μ EH c
 $C_{y,s,t}^{\text{Electricity}}$ Electricity tariff for IENGDS operator
 $C_{y,s}^{\text{Gas}}$ Natural gas tariff for IENGDS operator
 $Z_{i,j}$ Impedance of line i, j
 $\theta_{i,j}$ Admittance angle between buses i, j
 $P_{i,j}^{\text{Max}}$ Capacity of line i, j
 $K_{n,m}$ Weymouth constant of pipeline n, m
 $f_{n,m}^{\text{Max}}$ Capacity of gas pipeline n, m
 $\rho_n^{\text{Min}}, \rho_n^{\text{Max}}$ Lower and upper limit pressure of natural gas node n
 $\lambda_{n,m}^{\text{com}}$ Compressor factor at pipeline n, m

$\alpha_{n,m}^{\text{com.}}$	Fuel consumption factor of a natural gas compressor at pipeline n, m
$P_{y,s,t,i,sc}^{\text{Load}_{\text{net}}}$	Electricity demand of an electricity network
$P_{\text{sub.}}^{\text{Max}}$	Maximum imported electricity to the substation
$G_{y,s,t,n,sc}^{\text{Load}_{\text{net}}}$	Gas demand of a natural gas system
$G_{\text{source}}^{\text{Max}}$	Maximum imported natural gas from the gas wells to natural gas nodes

Variables

OC_c	Operation cost of $\mu\text{EH } c$
IC_c	Investment cost of $\mu\text{EH } c$
OC^{IENGDS}	IENGDS operation cost at planning horizon
$P_{y,s,t,c}^{\mu\text{EH}}, G_{y,s,t,c}^{\mu\text{EH}}$	Electricity and natural gas transferred to $\mu\text{EH } c$
$\text{Cap}_c^{\text{Boiler}}$	Installed boiler capacity at $\mu\text{EH } c$
$\text{Cap}_c^{\text{CHP}}$	Installed CHP capacity at $\mu\text{EH } c$
$\text{Cap}_c^{\text{ESS}}$	Installed ESS capacity at $\mu\text{EH } c$
N_c^{PV}	Number of installed 1-kW PV panels in each μEH
$P_{y,s,t,c,sc}^{\text{CHP}}$	Electricity generation of CHP at $\mu\text{EH } c$
$df_{y,s,t,c,sc}$	Dispatch factor of natural gas at $\mu\text{EH } c$
$H_{y,s,t,c,sc}^{\text{CHP}}$	Heat generation of CHP at $\mu\text{EH } c$
$H_{y,s,t,c,sc}^{\text{Boiler}}$	Heat generation of boiler at $\mu\text{EH } c$
$P_{y,s,t,c,sc}^{\text{chESS}}$	Charging energy of ESS at $\mu\text{EH } c$
$P_{y,s,t,c,sc}^{\text{dchESS}}$	Discharging energy of ESS at $\mu\text{EH } c$
$\text{SOC}_{y,s,t,c,sc}^{\text{ESS}}$	State of charge of ESS at $\mu\text{EH } c$
$P_{y,s,t,c,sc}^{\text{PV}}$	Produced energy by the PV panel at $\mu\text{EH } c$
$P_{y,s,t,i,\text{substation}}^{\text{Net}}$	Imported electricity to the substation
$G_{y,s,t,w_n}^{\text{Net}}$	Imported natural gas from gas wells
$P_{y,s,t,i,j}^i$	Active power flow through line i, j
$V_{y,s,t,i,sc}$	Voltage of the i^{th} bus
$\delta_{y,s,t,i,sc}$	Phase angle of the i^{th} bus
$f_{y,s,t,n,m,sc}$	Gas flow of gas pipeline
$\rho_{y,s,t,n,sc}$	Gas pressure of the n^{th} node
$I_{i,c}$	Binary decision variable for optimal place $\mu\text{EH } c$ in the electricity network
$II_{n,c}$	Binary decision variable for optimal place $\mu\text{EH } c$ in the natural gas system

I. INTRODUCTION

A. Research Background and Motivation

Electricity and natural gas systems are known as the most important energy infrastructures in the world. It is becoming popular to integrate the operation of different energy infrastructures [1], [2], due to the constantly growing energy demands, environmental concerns, and the rapid improvement of cogeneration technologies such as combined heat and power (CHP) units. Recent studies have shown that the integrated energy systems can increase the overall efficiency of energy consumption by approximately 20% [3], [4]. Accordingly, the operation and planning studies of the integrated electricity and natural gas distribution systems (IENGDSs) have become particularly

important. The optimal operation of multicarrier energy systems determines the optimal power flow of integrated energy systems, and thereby the amount of energy for each carrier should be purchased and converted to supply the energy demands [5]–[8]. Further, multicarrier energy systems planning studies seek to determine the optimal capacities of the components for a definite planning horizon [9]–[11]. These energy system operation and planning problems are usually solved through an optimization-based procedure [12].

Planning problems of integrated energy systems can be studied in two ways. First, from the customer viewpoint, where a customer may determine the optimal size and technology of IENGDS components such as CHP, boiler, renewable energy resources (RERs), and storage systems to provide heat and electricity demands with the lowest cost in a definite planning horizon. The multicarrier energy customer hereinafter is called the microenergy hubs (μEHs) operator. At the customer level, previous studies [13]–[18] tried to determine the optimal capacities of μEH components including CHP, boiler, energy storage, and RER. For example, the authors in [13] determined the optimal size of a single residential μEH , consisting of CHP, boiler, photovoltaic (PV) panel, and energy storage system (ESS), by minimizing the operation cost and installation cost during the planning horizon. The authors in [16] determined the optimal size and operation of the CHP, heat pump, absorption chiller, boiler, renewables, and ESS for residential μEH , by minimizing the investment, operational and maintenance costs, and the total carbon emissions during the planning horizon. Recent studies have modeled the uncertainties in energy demands [6], [10], [14], [19], [20], energy prices [10], and RERs (e.g., generation from PV panels [10], [13], [15], [19] and wind turbines [6], [14], [15], [20]), for μEH planning. For example, the authors in [14] proposed a probabilistic model to determine the optimal size of a wind turbine and μEH components including CHP, boiler, chiller, electrical and thermal storages, considering the uncertainties in wind power generation, and electricity and heat demands. The authors in [19] determined the optimal planning of a residential μEH including a CHP unit, ESS, PV, heater, electric heat pump, boiler, and absorption chiller, to minimize investment and operation costs, considering the demand response and uncertainties in PV power generation and energy demands.

On the other hand, the integrated energy system (i.e., IENGDS) operator may have various technical and economic concerns in system planning. These concerns should also be considered during the planning from the IENGDS operator viewpoint [21]–[25]. For instance, the authors in [21] focused on determining the optimal places and sizes of PV panels, heat boiler, and heat pumps in the coupled electricity and heating distribution systems, by minimizing the total purchased energy costs and the cost of electricity distribution losses. The authors in [22] tried to determine the optimal design of an urban integrated energy system, consisting of electricity, natural gas, and district heating systems, by minimizing the total costs, wind power curtailment, and variance of peak-valley electricity demands. The authors in [23] proposed a two-stage planning approach to determine the optimal site and size of CHPs in an IENGDS, by minimizing incremental network investment costs and use-of-system charges for IENGDS. The authors in [26] determined the optimal size and placement of CHP, using particle swarm

optimization. The objective is to reduce power losses and improve the voltage profile and reliability of microgrids. The authors in [27] tried to determine the optimal site and size of PV, CHP, heat and electricity storage in an integrated heat and electricity distribution network, by maximizing the economic profit of the system operator. Furthermore, some works considered seasonal studies on energy demands, prices, and RER output in planning optimization problems [13], [15], [17], [19], [24]. For instance, the authors in [24] determined the optimal placement of CHP, boiler, ESS, and wind turbine for an IENGDS, considering seasonal climate change and its effect on energy demands and prices, with an objective of minimizing the operation cost of the IENGDS.

Recent works [28]–[31] have used hierarchical and bilevel programming to consider both μ EH operators' and IENGDS operators' concerns in planning studies, while also keeping the privacy of μ EHs. For example, the authors in [29] investigated the interaction between the heating costs of end-users in winter and energy generation of components such as CHP, power to gas units, and gas boiler. The upper level maximized the benefits of the energy supplier while the lower level minimized the heating costs of customers. The authors in [31] proposed a bilevel linear problem to determine the optimal operation of μ EHs in IENGDS, in which each μ EH was operated by a specific operator with its own objective function. In [31], the objective of μ EH operators and the IENGDS operator was minimized simultaneously. The authors in [32] proposed bilevel planning for an integrated electricity and heating distribution system, considering a demand response program. In the lower level, the optimal sizes of ESS, heat boiler, and RER were determined by minimizing the installation and operation costs of μ EH. Then, the upper level optimized the operation of electricity and heating systems during the planning horizon, by minimizing the operation cost of the integrated energy system. The uncertainties in the power generation of wind turbines and PV panels, and energy demands were also considered under different scenarios.

Previous works in integrated energy systems focused on customer-level problems [13], [19] or distribution networks for equipment sizing and placement [21], [23], [24], [26]. Although recent works considered concerns of both μ EH and IENGDS operators [29]–[32], the impacts of μ EHs' location on the system performance have not been studied in the literature. It should be noted that, if system operators estimate and declare their housing capacities, μ EH operators will be forced to select the specified capacity. Moreover, if the system operator estimates capacities of μ EHs, then optimal conditions from the system operator viewpoint may not be met. Fig. 1 shows the overall concept of μ EH placement in an IENGDS, where multiple candidate electricity network buses and natural gas nodes could potentially connect to a μ EH. An optimal placement study aims to determine the best nodes and busses for the μ EH establishment. In this study, the hierarchical model is proposed for optimal sizing and placement of μ EHs in an IENGDS to determine the optimal capacity of μ EHs components and the optimal locations of μ EHs in an IENGDS. In the hierarchical optimization problems, there are two (or more) agents in one problem, where each of them is responsible for optimizing their own objective(s). The hierarchical problems can have more advantages compared to the single-level optimization problems

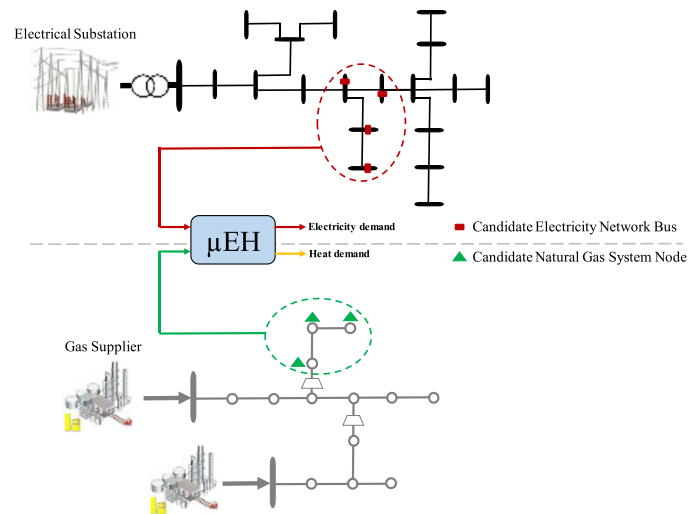


Fig. 1. Placement of μ EH in an IENGDS.

from a single operator's viewpoint in previous works. The reason is that if the optimization process is done simultaneously from a single operator's viewpoint, then the optimization results may not be in line with the goals of other operators. Furthermore, in hierarchical problems, the computational burden decreases compared to single-level problems, because the IENGDS does not consider complicated details of μ EHs schedules.

B. Research Objective

To address the μ EH locating challenge, this article formulates a hierarchical probabilistic planning problem for optimal locating and structural sizing of multiple μ EHs in a distribution energy system. Fig. 2 shows the overall framework of the proposed IENGDS and μ EH planning problem, where the optimal sizes of μ EH components are first determined, and then, the optimal locations of μ EHs are determined. In the first step, from the μ EH operator viewpoint, the optimal size of a CHP, a boiler, an ESS, and PV panels are determined in each μ EH by solving an optimization problem. The objective of the μ EH operator is to minimize the operation and investment costs in the planning horizon. Load-dependent CHP exchange efficiencies are also considered to model μ EH operation; the input energy of μ EHs and the optimal operation of μ EH components are scheduled by considering the operational constraints of μ EHs. Since the IENGDS operator only receives the required energy of μ EHs, the privacy of μ EHs and details of the first step operation are preserved. In the second step, the main goal of the IENGDS operator is to determine μ EHs' optimal locations, i.e., the electricity network buses and the natural gas nodes, to connect each μ EH to the IENGDS. The optimal power flow and gas flow in IENGDS are also determined by solving an optimization problem, considering the operational and technical constraints of the energy systems. The objective of the second step is to minimize the operation costs of IENGDS that consist of the purchased electricity and natural gas from the upstream network during the planning horizon. It is also important to note that, the proposed hierarchical planning problem is modeled by considering different energy tariffs to represent seasonal

TABLE I
COMPARING DIFFERENT STUDIES WITH PRESENT WORK

Reference	Field of study (Operation/ Planning)	Viewpoint of problem (System operator/ Customer)	Uncertainty modeling	Load dependent CHP conversion efficiency	μ EH siting	Planned components			
						CHP	Boiler	ESS	RERs
[13]	Planning	Customer	✓	✓	✗	✓	✓	✓	✓
[18]	Planning	Customer	✓	✗	✗	✓	✓	✓	✗
[19]	Planning	Customer	✓	✓	✗	✓	✓	✓	✓
[21]	Planning	System operator	✗	✗	✓	✓	✓	✗	✓
[24]	Planning	System operator	✗	✗	✓	✓	✓	✓	✓
[26]	Planning	System operator	✗	✗	✓	✓	✗	✗	✗
[30]	Operation	Hierarchical	✗	✗	✗	✓	✓	✓	✗
[31]	Operation	Hierarchical	✗	✗	✗	✓	✓	✗	✓
[32]	Planning	Hierarchical	✓	✗	✗	✗	✓	✓	✓
Present work	Planning	Hierarchical	✓	✓	✓	✓	✓	✓	✓

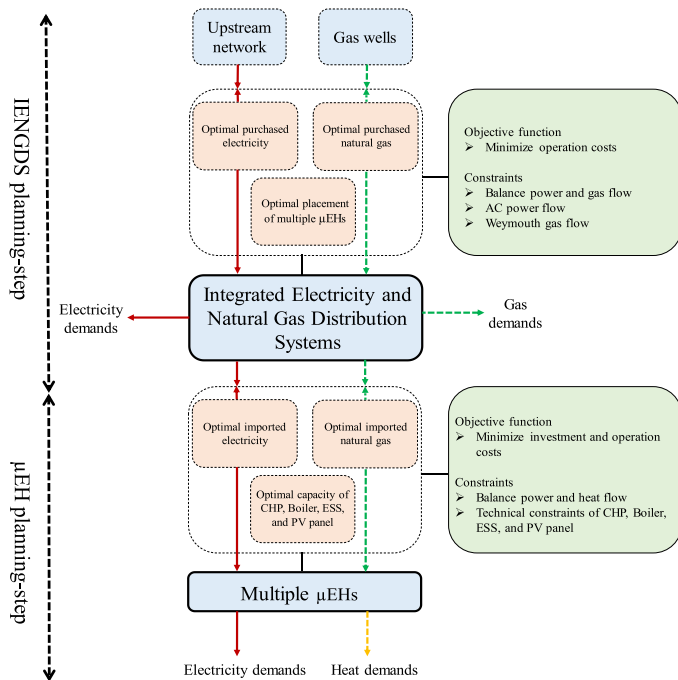


Fig. 2. Overall framework of the proposed IENGDS and μ EH planning problem.

variations in the electricity, heating, gas demands, and PV panel output; and a two-stage stochastic programming framework is developed to model and manage the uncertainties in energy demands and PV generation. Table I shows the taxonomy of the similar studies in the literature for the system operator and customers. The differences between the proposed model and previous works are specified.

The main contributions of this article are as follows.

- 1) A hierarchical planning model is proposed to obtain the optimal sizing and placement of μ EHs in the IENGDS.
- 2) The two-stage stochastic programming framework is employed in the hierarchical planning model optimization to evaluate uncertain parameters of energy demands and renewable energy resources.

TABLE II
LOCATIONS OF μ EHs IN THE IENGDS UNDER DIFFERENT CASES

	Electricity network buses	Natural gas nodes
Case 1	μ EH1 μ EH2 μ EH3 Optimal buses	Optimal nodes
Case 2	μ EH1 μ EH2 μ EH3 12 33 17	Optimal nodes
Case 3	μ EH1 μ EH2 μ EH3 Optimal buses	16 13 20

3) Seasonal climate change and its effect on energy consumption have been considered in μ EH and IENGDS planning.

The rest of the article is organized as follows. Section II formulates the proposed IENGDS and μ EH models, and presents the two-stage stochastic programming framework. Section III discusses the results of a case study with an IENGDS that consists of the IEEE 33-bus electricity distribution test system and the Belgian 20-node natural gas system. Finally, Section IV concludes the study and discusses potential future work.

II. IENGDS AND μ EH MODELING AND STOCHASTIC PLANNING FORMULATION

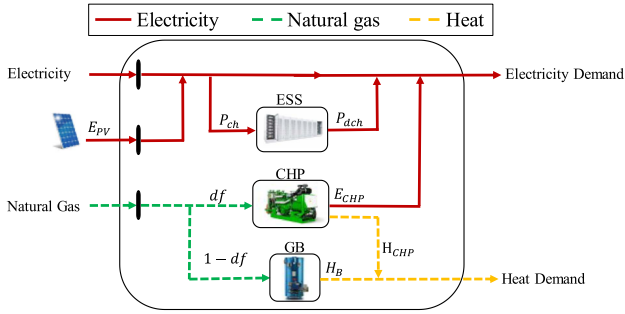
The formulation of the proposed method consists of two steps: the μ EH planning step and the IENGDS planning step.

A. μ EH Planning Problem Formulation

Fig. 3 presents the proposed μ EH structure that consists of a CHP unit, an ESS, a gas boiler, and a PV panel. The main goal of the μ EH operator is to determine the optimal capacities of μ EH components; the purchased electricity and natural gas from IENGDS are also determined at this step.

Equations (1)–(3) formulate the objective function of the μ EH planning problem, seeking to minimize the total costs of each μ EH that consist of the investment cost (IC) of the newly installed components and the operation cost (OC) of purchasing energy from the distribution system during the planning horizon.

$$\text{Min } \text{obj} = \text{OC}_c + \text{IC}_c \quad \forall c \in \mu\text{EH} \quad (1)$$

Fig. 3. Overall structure of the μ EH.

$$\begin{aligned}
 OC_c &= \sum_{y,s,t} (ND_s C_{y,s,t}^{\mu EH \text{electricity}} P_{y,s,t,c}^{\mu EH}) \\
 &+ \sum_{y,s,t} (ND_s C_{y,s,t}^{\mu EH \text{gas}} G_{y,s,t,c}^{\mu EH}) \quad \forall c \in \mu EH \\
 IC_c &= C^{\text{CHP}} \text{Cap}_c^{\text{CHP}} + C^{\text{Boiler}} \text{Cap}_c^{\text{Boiler}} \\
 &+ C^{\text{ESS}} \text{Cap}_c^{\text{ESS}} + C^{\text{PV}} N_c^{\text{PV}}, \quad \forall c \in \mu EH.
 \end{aligned} \quad (2)$$

Equation (2) denotes the operation cost of purchasing energy from the IENGDS operator during the planning horizon, and (3) considers the installation costs of the CHP, boiler, ESS, and PV panel. Equations (4)–(19) formulate the constraints of the μ EH planning problem

$$P_{y,s,t,c,sc}^{\text{CHP}} = df_{y,s,t,c,sc} G_{y,s,t,c}^{\mu EH} \eta_{y,s,t,c,sc}^{ge\text{CHP}}, \quad \forall y \forall s \forall t \forall c \in \mu EH \forall sc \quad (4)$$

$$H_{y,s,t,c,sc}^{\text{CHP}} = P_{y,s,t,c,sc}^{\text{CHP}} / \beta_{y,s,t,c,sc}^{ph\text{CHP}} \quad \forall y \forall s \forall t \forall c \in \mu EH \forall sc \quad (5)$$

$$PL_{y,s,t,c,sc}^{\text{CHP}} = P_{y,s,t,c,sc}^{\text{CHP}} / \text{Cap}_c^{\text{CHP}} \quad \forall y \forall s \forall t \forall c \in \mu EH \forall sc \quad (6)$$

$$\begin{aligned}
 \eta_{y,s,t,c,sc}^{ge\text{CHP}} &= 0.9033(PL_{y,s,t,c,sc}^{\text{CHP}})^5 - 2.9996(PL_{y,s,t,c,sc}^{\text{CHP}})^4 \\
 &+ 3.6503(PL_{y,s,t,c,sc}^{\text{CHP}})^3 - 2.0704(PL_{y,s,t,c,sc}^{\text{CHP}})^2 \\
 &+ 0.4623PL_{y,s,t,c,sc}^{\text{CHP}} + 0.3747 \\
 &\quad \forall y \forall s \forall t \forall c \in \mu EH \forall sc
 \end{aligned} \quad (7)$$

$$\begin{aligned}
 \beta_{y,s,t,c,sc}^{ph\text{CHP}} &= 1.0785(PL_{y,s,t,c,sc}^{\text{CHP}})^4 - 1.9739(PL_{y,s,t,c,sc}^{\text{CHP}})^3 \\
 &+ 1.5005(PL_{y,s,t,c,sc}^{\text{CHP}})^2 - 0.2817PL_{y,s,t,c,sc}^{\text{CHP}} \\
 &+ 0.6838 \quad \forall y \forall s \forall t \forall c \in \mu EH \forall sc
 \end{aligned} \quad (8)$$

$$H_{y,s,t,c,sc}^{\text{Boiler}} = (1 - df_{y,s,t,c,sc}) G_{y,s,t,c}^{\mu EH} \eta_c^{\text{Boiler}} \quad \forall y \forall s \forall t \forall c \in \mu EH \forall sc \quad (9)$$

$$H_{y,s,t,c,sc}^{\text{Load}\mu EH} = H_{y,s,t,c,sc}^{\text{Boiler}} + H_{y,s,t,c,sc}^{\text{CHP}} \quad \forall y \forall s \forall t \forall c \in \mu EH \forall sc \quad (10)$$

$$\begin{aligned}
 &P_{y,s,t,c,sc}^{\text{CHP}} + P_{y,s,t,c,sc}^{\text{dchESS}} + P_{y,s,t,c}^{\text{EH}} + P_{y,s,t,c,sc}^{\text{PV}} \\
 &= P_{y,s,t,c,sc}^{\text{Load}\mu EH} + P_{y,s,t,c,sc}^{\text{chESS}} \\
 &\quad \forall y \forall s \forall t \forall c \in \mu EH \forall sc
 \end{aligned} \quad (11)$$

$$\begin{aligned}
 \text{SOC}_{y,s,t,c,sc}^{\text{ESS}} &= \text{SOC}_{y,s,t-1,c,sc}^{\text{ESS}} + P_{y,s,t,c,sc}^{\text{chESS}} \eta^{\text{ch}} \\
 &- P_{y,s,t,c,sc}^{\text{dchESS}} / \eta^{\text{dch}} \\
 &\quad \forall y \forall s \forall t \forall c \in \mu EH \forall sc
 \end{aligned} \quad (12)$$

$$P_{y,s,t,c,sc}^{\text{chESS}} \leq P_{\text{ch}}^{\text{Max}}, \quad P_{y,s,t,c,sc}^{\text{dchESS}} \leq P_{\text{dch}}^{\text{Max}} \quad \forall y \forall s \forall t \forall c \in \mu EH \forall sc \quad (13)$$

$$\text{SOC}_{y,s,24,c,sc}^{\text{ESS}} \leq \text{SOC}_0^{\text{ESS}} \quad \forall y \forall s \forall t \forall c \in \mu EH \forall sc \quad (14)$$

$$P_{y,s,t,c}^{\mu EH} \leq P_{\text{Input}\mu EH}^{\text{Max}}, \quad G_{y,s,t,c}^{\mu EH} \leq G_{\text{Input}\mu EH}^{\text{Max}} \quad \forall y \forall s \forall t \forall c \in \mu EH \quad (15)$$

$$N_c^{\text{PV}} P_{s,t,sc}^{\text{PVbase}} \leq P_{y,s,t,c,sc}^{\text{PV}} \quad \forall y \forall s \forall t \forall c \in \mu EH \forall sc \quad (16)$$

$$P_{y,s,t,c,sc}^{\text{CHP}} \leq \text{Cap}_c^{\text{CHP}} \quad \forall y \forall s \forall t \forall c \in \mu EH \forall sc \quad (17)$$

$$H_{y,s,t,c,sc}^{\text{Boiler}} \leq \text{Cap}_c^{\text{Boiler}} \quad \forall y \forall s \forall t \forall c \in \mu EH \forall sc \quad (18)$$

$$\text{SOC}_{y,s,t,c,sc}^{\text{ESS}} \leq \text{Cap}_c^{\text{ESS}} \quad \forall y \forall s \forall t \forall c \in \mu EH \forall sc. \quad (19)$$

Constraints (4)–(9) denote the output energy of CHP and boiler that depends on the dispatch factor (df), gas-to-power (G2P) efficiency, power-to-heat (P2H) ratio, and boiler efficiency. The dispatch factor determines how the purchased gas is distributed between the CHP and the boiler. The part load ratio of CHP is expressed in (6), using $\eta_{y,s,t,c,sc}^{ge\text{CHP}}$ and $\beta_{y,s,t,c,sc}^{ph\text{CHP}}$ coefficients from (7) and (8), respectively. If $PL_{y,s,t,c,sc}^{\text{CHP}} \geq 0.05$, constraints (7) and (8) are valid; or else $\eta_{y,s,t,c,sc}^{ge\text{CHP}}$ and $\beta_{y,s,t,c,sc}^{ph\text{CHP}}$ are assumed to be 0.2716 and 0.6816, respectively [33]. Equations (10) and (11) denote the heat and electricity balance in all μ EHs, respectively. Electricity demands can be supplied by CHP, ESS, PV generation, and electricity purchased from the grid; heat demands can be satisfied by CHP and boiler. The operational constraints of ESS are formulated in (12)–(14). Equation (12) represents the state of charge (SOC) of the ESS that depends on the SOC at the previous hour, the efficiency, charging, and discharging rate at each hour. Equation (13) denotes the maximum charging and discharging rates of ESS. Equation (14) represents that the SOC at the end of a day, which should be more than or equal to the ESS initial SOC. The upper limits for imported electricity and natural gas at each μ EH are expressed in (15). Equation (16) ensures that the produced electricity from PV at each μ EH should be less than its maximum capacity. In this article, the energy profiles of 1-kW PV panel in each season are employed as the base data in the optimization. Therefore, the optimization process determines the optimal number of PV panels (N_h^{PV}) and the output electricity at each μ EH. Equations (17)–(19) guarantee that the output energy of CHP, boiler, and ESS cannot be more than their nominal capacities.

B. IENGDS Planning Problem Formulation

The objective function of the IENGSD planning problem is formulated in (20). In the IENGSD planning step, the best electricity buses and natural gas nodes are determined for installing μ EHs, by minimizing the operation cost of IENGDS, i.e., the purchased electricity from the upstream network and the purchased natural gas from wells over the planning period

$$\begin{aligned} \text{Min obj} &= OC^{\text{IENGDS}} \\ &= \sum_{y,s,t} (ND_s C_{y,s,t}^{\text{Electricity}} P_{y,s,t,i_{\text{substation}}}^{\text{Net}}) \\ &\quad + \sum_{\substack{y,s,t \\ w_n \in \Omega_G}} (ND_s C_{y,s,t}^{\text{Gas}} G_{y,s,t,w_n}^{\text{Net}}). \end{aligned} \quad (20)$$

Equations (21)–(35) describe the optimization constraints of the IENGDS planning problem

$$\begin{aligned} P_{ij,y,s,t,i,j,sc} &= \frac{V_{y,s,t,i,sc}^2}{Z_{i,j}^2} \cos(\theta_{i,j}) \\ &\quad - \frac{V_{y,s,t,i,sc} V_{y,s,t,j,sc}}{Z_{i,j}} \cos(\delta_{y,s,t,i,sc} - \delta_{y,s,t,j,sc} + \theta_{i,j}) \\ &\quad \forall y \forall s \forall t \forall i, j \in \Omega_B \forall sc \end{aligned} \quad (21)$$

$$0.9^{p.u.} \leq V_{y,s,t,i,sc} \leq 1.1^{p.u.}, \quad -\frac{\pi}{2} \leq \delta_{y,s,t,i,sc} \leq \frac{\pi}{2} \quad \forall y \forall s \forall t \forall i, j \in \Omega_B \forall sc \quad (22)$$

$$\begin{aligned} V_{y,s,t,i_{\text{substation}}} &= 1^{p.u.}, \delta_{y,s,t,i_{\text{substation}}} \\ &= 0 \quad \forall y \forall s \forall t \forall i_{\text{substation}} \in \Omega_B \end{aligned} \quad (23)$$

$$\begin{aligned} -P_{i,j}^{\text{Max}} &< P_{ij,y,s,t,i,j,sc} < P_{i,j}^{\text{Max}} \\ &\quad \forall y \forall s \forall t \forall i, j \in \Omega_B \forall sc \end{aligned} \quad (24)$$

$$\begin{aligned} f_{y,s,t,n,m,sc}^2 + (K_{n,m} \rho_{y,s,t,m,sc})^2 &\leq (K_{n,m} \rho_{y,s,t,n,sc})^2 \\ &\quad \forall y \forall s \forall t \forall n, m \in \Omega_N \forall sc \end{aligned} \quad (25)$$

$$0 \leq f_{y,s,t,n,m,sc} \leq f_{n,m}^{\text{Max}}, \quad \rho_n^{\text{Min}} \leq \rho_{y,s,t,n,sc} \leq \rho_n^{\text{Max}} \quad \forall y \forall s \forall t \forall n, m \in \Omega_N \forall sc \quad (26)$$

$$\begin{aligned} \rho_{y,s,t,m,sc} \leq \rho_{y,s,t,n,sc}, \quad \rho_{y,s,t,m,sc} &\leq \lambda_{n,m}^{\text{com}} \rho_{y,s,t,n,sc} \\ &\quad \forall y \forall s \forall t \forall n, m \in \Omega_N \forall sc \end{aligned} \quad (27)$$

$$\begin{aligned} P_{y,s,t,i_{\text{substation}}}^{\text{Net}} - P_{y,s,t,i,sc}^{\text{Load,net}} - I_{i,c} P_{y,s,t,c}^{\mu EH} \\ = \sum_j P_{ij,y,s,t,i,j,sc} \end{aligned} \quad \forall y \forall s \forall t \forall i, j \in \Omega_B \forall c \in \mu EH \forall sc \quad (28)$$

$$\begin{aligned} G_{y,s,t,w_n}^{\text{Net}} - G_{y,s,t,n,sc}^{\text{Load,net}} - II_{n,c} G_{y,s,t,c}^{\mu EH} \\ = \sum_{v(n,m)} f_{y,s,t,v(n,m),sc} \\ + \sum_{v(n,m)} \alpha_{n,m}^{\text{com}} f_{y,s,t,v(n,m),sc} - \sum_{v(g,n)} f_{y,s,t,v(g,n),sc} \\ \quad \forall y \forall s \forall t \forall n, m, g \in \Omega_N \forall w_n \in \Omega_G \forall c \in \mu EH \forall sc \end{aligned} \quad (29)$$

$$P_{y,s,t,i_{\text{substation}}}^{\text{Net}} \leq P_{\text{sub}}^{\text{Max}} \quad \forall y \forall s \forall t \forall i_{\text{substation}} \in \Omega_B \quad (30)$$

$$G_{y,s,t,w_n}^{\text{Net}} \leq G_{\text{source}}^{\text{Max}} \quad \forall y \forall s \forall t \forall w_n \in \Omega_G \quad (31)$$

$$\sum_i I_{i,c} = 1 \quad \forall c \in \mu EH \quad (32)$$

$$I_{i,c} \times I_{i,e} = 0 \quad \forall i \in \Omega_B \forall c, e \in \mu EH \forall c \neq e \quad (33)$$

$$\sum_n II_{n,c} = 1 \quad \forall c \in \mu EH \quad (34)$$

$$II_{n,c} \times II_{n,e} = 0 \quad \forall n \in \Omega_N \forall c, e \in \mu EH \forall c \neq e. \quad (35)$$

In (21), ac active power flow is adopted in the electricity network. Equations (22)–(24) represent the minimum and maximum ranges of voltage, angle of each bus, and electricity within the lines, respectively. Constraint (25) imposes the Weymouth equation for the operation condition of the natural gas system, which represents the relationship between gas flow within pipelines and nodes gas pressure. The Weymouth constant of pipeline depends on the pipe diameter and line length [34], [35]. Equation (26) ensures that the gas flow and gas pressure should be within predefined ranges. The flow directions in the natural gas system and the maximum natural gas compression ratio are given in (27). The energy balance in IENGDS is formulated in (28) and (29). Equation (28) represents the active power balance of the electricity network; the upstream network can supply the electricity to be transferred to μ EHs and each load bus. Equation (29) represents the nodal natural gas balance among the imported gas from the gas wells, the gas flow through pipelines, the gas load of each node, and the gas to be transferred to each μ EH. It should be mentioned that electricity and natural gas inputs of μ EHs can be obtained from the first step of the optimization problem (i.e., the μ EH planning problem). Moreover, binary variables in (28) and (29) could be used to optimize the site selection of μ EHs in the IENGDS, where $I_{i,h}$ and $II_{n,h}$, respectively, denote binary variables of the optimal locations in the electricity network and the natural gas system. The maximum allowable purchased electricity from the upstream network and the imported gas from gas wells are represented in (30) and (31), respectively. Constraints (32)–(35) enforce the optimal placement of the μ EHs in the IENGDS. Equation (32) ensures that each μ EH can only be connected to one electricity network bus; equation (34) ensures that each μ EH should be installed at one natural gas node; equations (33) and (35) eliminate certain locations for μ EHs. Thus, according to constraints (28)–(29) and (32)–(35), constraints of candidate nodes have been reflected in the modeling.

C. Two-Stage Stochastic Programming Planning Framework

Several methods exist in the literature for uncertainty quantification and modeling. For example, the authors in [36] modified a two-point estimation method to consider the uncertainties related to energy demands, wind and PV generation. The authors in [20], modeled the uncertain parameters of the energy demands and wind turbine generation, by employing information gap decision theory and interval method. The authors in [19] used two-stage stochastic programming in the optimal planning of a residential μ EH to model uncertainties in energy demands and PV generation. In this article, the uncertainties in the electricity, heat, gas demands, and PV generation are considered in a two-stage stochastic programming model. In particular, in the two-stage

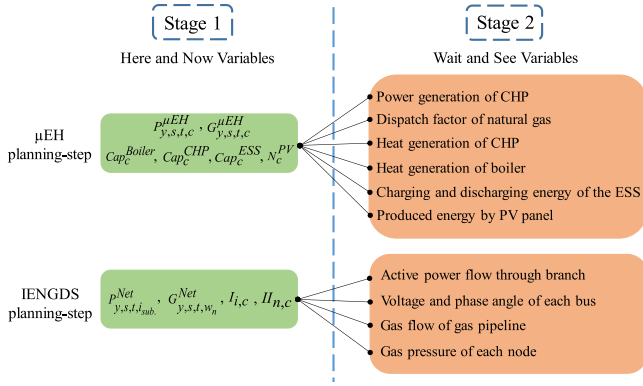


Fig. 4. Variables in the two-stage stochastic programming framework.

stochastic programming, design variables and operational variables can be decided in different stages of the planning problem. Two-stage stochastic programming can be used in various fields, such as supply chain planning, process design, and operation and infrastructure planning. The most important advantage of this technique is the ability to find optimal solutions for large-scale planning problems [37]. To this end, different scenarios are generated by using Monte Carlo simulations (MCS). A Gaussian distribution is employed for generating several scenarios, and a 5% standard deviation is applied to generate each scenario. The two-stage stochastic programming model divides all the design variables into two groups. The first-stage variables, which are called “here and now variables,” are deterministic parameters, which do not change in different probabilistic scenarios during the planning horizon. The second-stage variables, which are called “wait-and-see variables,” include the rest of variables that are flexible in probabilistic scenarios [38]–[40]. In this article, the first-stage variables include imported energy to μ EHs from IENGDS, imported energy to IENGDS from the upstream network and gas wells, and investment decisions, i.e., the optimal sizes and locations of μ EHs. The second-stage variables include operational decisions of μ EHs and IENGDS during the planning horizon. Fig. 4 shows the variables of the hierarchical two-stage stochastic programming problem in each stage.

III. NUMERICAL STUDIES

A test IENGDS, that consists of the IEEE 33-bus electricity network and the Belgian 20-node natural gas system, is adopted for numerical studies. It is assumed that the IENGDS operator needs to determine the optimal locations of three different μ EHs, i.e., the optimal electricity network buses and natural gas nodes for connecting μ EHs; the μ EH operator is responsible for the optimal component capacities and daily operation schedules of μ EHs. To evaluate the effectiveness of the proposed model, three cases are defined and compared.

- *Case 1: (Proposed Optimal Case)*: By following the proposed framework, the μ EHs components and daily operations are first optimized by the μ EH operator, and then the optimal μ EHs locations are determined by the IENGDS operator. Both the capacities of μ EHs components and the μ EHs locations are optimized in this case.
- *Case 2*: The capacities of μ EHs components and the natural gas nodes connecting μ EHs are the same as those in Case

TABLE III
INVESTMENT COSTS OF μ EHs COMPONENTS [13]

Components	Investment cost (\$/kW)
CHP	750
Boiler	300
Electrical storage	500
PV panel	1000

1; however, the electricity network buses connecting μ EHs are different from those in Case 1. Case 2 is designed to show the importance of optimal electricity network buses in the procedure of optimal locating of μ EHs.

- *Case 3*: The electricity network buses are the same as those in Case 1, while different natural gas nodes are considered.

In summary, Table II shows the Case studies. Cases 2 and 3 are in line with previous works [21], [23], [24], [26] that optimal μ EH sizing and placement were determined in single-level optimization problems from a single operator’s viewpoint.

The model of the μ EH planning-step is solved using the interior point optimizer (IPOPT) solver that is a nonlinear programming (NLP) solver. The IENGDS planning step is solved using the basic open-source nonlinear mixed integer programming (BONMIN) solver that is a mixed-integer nonlinear programming (MINLP) solver [11], [41]. It should be mentioned that, since our proposed model is a planning problem, computational speed is not our first priority in comparison with accuracy and optimality. Thus, integer variables have been added to the proposed model. The problems are solved under the global algebraic modeling system (GAMS) environment, using a core i7, 3.7-GHz processor, and 48-GB RAM.

A. Assumptions

The planning horizon is assumed to be 10 a. The investment costs of μ EH components are summarized in Table III. It should be mentioned that the economic life of μ EH components is more than 10 a [42]–[45]. Thus, the economic life of μ EH components in the proposed model is more than the planning horizon of this study, and we can ignore the end-of-life prices and replacement costs. The electricity tariff, i.e., the price of selling electricity from the upstream network to the IENGDS operator, is assumed to be a three-step time-of-use (TOU) tariff as illustrated in Fig. 5.

The gas tariff is constant during the day in each season, which is assumed to be \$80/MWh, \$50/MWh, \$80/MWh, and \$110/MWh for spring, summer, fall, and winter in year 1, respectively, by following [24]. Energy tariffs from the μ EH operator are \$10 more than those from the IENGDS operator. It should be mentioned that electricity and natural gas tariffs are increased by 7% and 5% annually, respectively. These values show the increase rate of energy tariffs during the planning horizon. Moreover, each 1 MWh is considered to be 3412 cubic feet (cf) of the natural gas system.

Figs. 6 and 7 show the base electricity and heat demands in different seasons [24]. In addition, Tables IV–VI present the load coefficients for μ EHs energy demands, electricity demand at each bus, and gas demand at each node in the IENGDS, respectively [30]. It should be mentioned that: 1) The energy demands of μ EHs at each hour are obtained by multiplying the

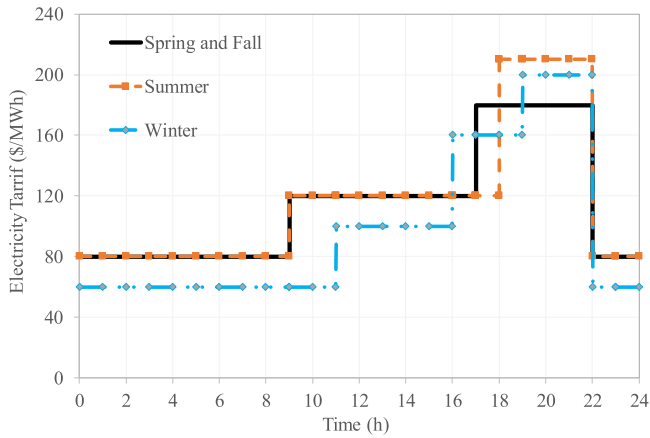


Fig. 5. Hourly wholesale electricity tariff in different seasons in year 1 [24].

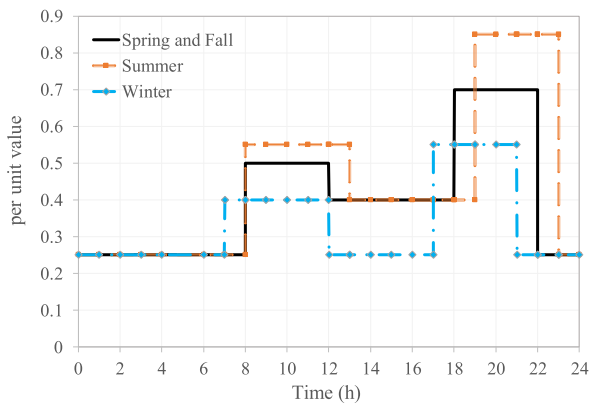


Fig. 6. Base electricity demand in different seasons [24].

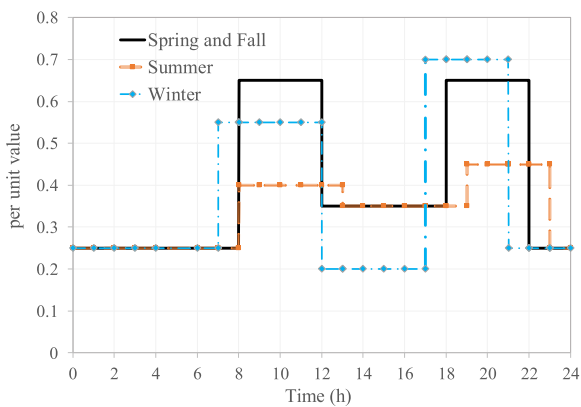


Fig. 7. Base heat demand in different seasons [24].

TABLE IV
LOAD COEFFICIENT FOR μ EH DEMANDS IN YEAR 1 [30]

μ EH	Electricity demand (MW)	Heat demand (MW)
1	0.35	0.4
2	0.4	0.3
3	0.5	0.5

TABLE V
LOAD COEFFICIENT FOR ELECTRICITY DEMANDS OF IENGDS BUSES IN YEAR 1 [30]

Bus	2	3	4	5	6	7	8	9
$P_{(MW)}^{Load_{net}}$	0.1	0.09	0.12	0.06	0.06	0.2	0.2	0.06
Bus	10	11	12	13	14	15	16	17
$P_{(MW)}^{Load_{net}}$	0.06	0.045	0.06	0.06	0.12	0.06	0.06	0.06
Bus	18	19	20	21	22	23	24	25
$P_{(MW)}^{Load_{net}}$	0.09	0.09	0.09	0.09	0.09	0.09	0.42	0.42
Bus	26	27	28	29	30	31	32	33
$P_{(MW)}^{Load_{net}}$	0.06	0.06	0.06	0.12	0.2	0.15	0.21	0.06

TABLE VI
LOAD COEFFICIENT FOR GAS DEMANDS OF IENGDS NODES IN YEAR 1 [30]

Node	2	3	4	6	7	10	11	12
$G_{(kef)}^{Load_{net}}$	4.94	5.46	2.41	3.91	3.28	5.63	3.62	3.22
Node	13	14	15	16	17	19	20	
$G_{(kef)}^{Load_{net}}$	4.37	2.93	3.33	4.54	4.19	3.28	2.36	

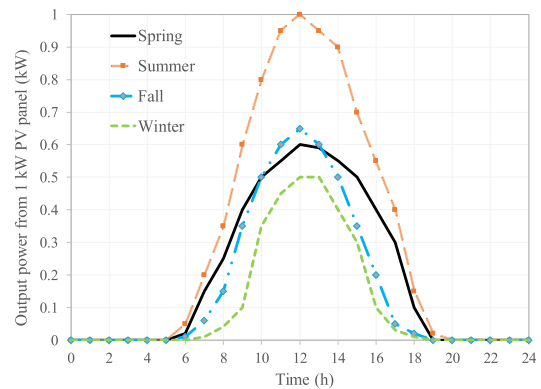


Fig. 8. Mean output power from the 1-kW PV panel in different seasons [46].

load coefficient in Table IV with the base electricity and heat demands; 2) the electricity demand of the electricity network at each bus is calculated by multiplying the load coefficient in Table V with the base electricity demand; 3) the natural gas demand at each node of the natural gas system is calculated by multiplying the load coefficient in Table VI with the base heat demand on a heat-to-gas conversion ratio (which is 0.95% in this article). Furthermore, the load coefficients of electricity, heat, and gas demands are increased by 7%, 5%, and 5% annually, respectively.

The conversion efficiency of the boiler is assumed to be 75%, and the ESS has a charging and discharging efficiency of 95%.

The output power of the 1-kW PV panel also varies in each season, and Fig. 8 shows the profiles of the mean PV power output in different seasons [46].

The IENGDS system configuration parameters are adopted from [30]. It is assumed that the IENGDS operator can determine candidate locations for μ EHs installation in consultation with the μ EH operators. Consequently, the IENGDS operator nominates several buses and nodes for installing each μ EH, considering

TABLE VII
CANDIDATE BUSES AND NODES FOR EACH μ EH PLACEMENT

	Electricity network bus	Natural gas node
μ EH1	5	7
	12	14
	26	16
μ EH2	21	13
	29	17
μ EH3	33	10
	12	3
	17	20
	24	13

TABLE VIII
OPTIMAL CAPACITIES OF μ EH COMPONENTS (kW)

	CHP	Boiler	ESS	PV
μ EH1	255	301	1007	337
μ EH2	306	173	1173	403
μ EH3	422	312	1296	470

the viewpoint of the μ EH operator. Therefore, the exact location is determined by solving the proposed optimization problem. Table VII lists the candidate buses and nodes of IENGDS. According to Table VII, each μ EH can choose one of the candidate buses and nodes to connect to IENGDS.

B. Simulation Results

By optimizing the sizes of μ EHs, it is found that the investment costs of μ EH1, μ EH2, and μ EH3 are \$1.1 million, \$1.3 million, and \$1.5 million, respectively. The operation costs of μ EH1, μ EH2, and μ EH3 are \$3.8 million, \$3.3 million, and \$4.9 million, respectively, during the planning horizon. Table VIII presents the optimal capacities of μ EH components. Since the electricity and heat demands in μ EH3 are higher than those in μ EH1 and μ EH2, the optimal capacities of the CHP, boiler, ESS, and PV panels are also larger. Moreover, the optimal capacities of the CHP, ESS, and PV panels in μ EH2 are more than those in μ EH1, due to the higher electricity demand in μ EH2 compared to μ EH1. However, the optimal capacity of the boiler in μ EH2 is smaller than that in μ EH1, due to the lower heat demand in μ EH2 compared to μ EH1. It is also observed from Tables IV and VIII that in the μ EHs, the capacity of CHP is increased with the increasing electricity demand. This is partially due to that CHPs generate heat and power simultaneously, and they play a key role in supplying the electricity and heat demands during the high tariff hours.

Fig. 9 shows the optimal electricity network buses and the optimal natural gas nodes for installing the μ EHs in Case 1 (optimal case). The operation cost of IENGDS is \$118.6 million during the planning horizon. It is found that the total operation cost is increased by \$367000 and \$110000 in Cases 2 and 3, respectively, compared to the optimal case. It is observed that the optimal locations of μ EHs are selected at the buses that are closer to the substation of the electricity network, due to the reduced power losses compared to installing μ EHs at the end of IENGDS. Fig. 10 compares the power line losses at a peak load hour (i.e., hour 20) of a typical summer day in different years,

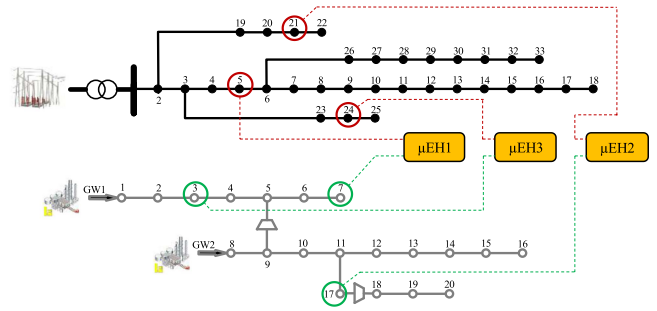


Fig. 9. Optimal locations of μ EHs in the IENGDS obtained in the proposed optimal case.

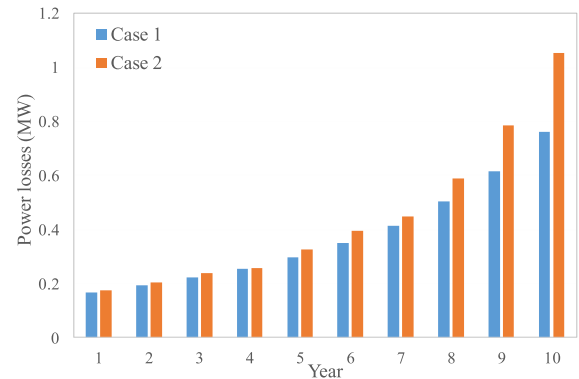


Fig. 10. Power losses through the lines at a peak load hour of a typical summer day in different years.

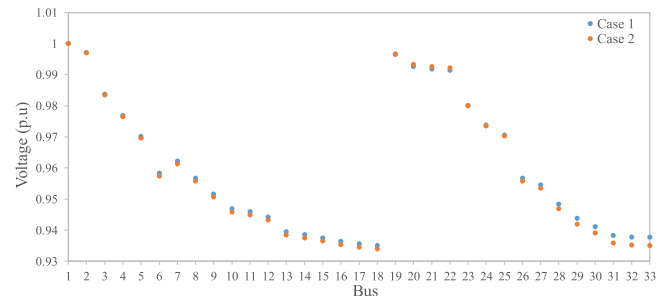


Fig. 11. Bus voltages at the peak load hour of a typical summer day in year 1.

between Case 1 and Case 2. Please note Case 3 has the same electricity network bus connections (i.e., same power losses) as Case 1. It is observed that Case 1 has 4% and 27.5% less power loss than Case 2 in Year 1 and Year 10, respectively. Thereby, the operation condition and total cost are improved at the IENGDS with the optimal μ EH placement.

Fig. 11 compares the voltage profile between Cases 1 and 2, during a typical summer day at peak load hour (i.e., hour 20) in year 1. Moreover, Table IX presents the voltages at buses 16, 17, 18, 31, 32, and 33 for a typical summer day at peak load hour in different years in Cases 1 and 2. It can be seen that the voltage profile in Case 1 is improved in comparison with Case 2. For example, at bus 33, the voltage amplitude is improved by 0.3%, 0.8%, and 0.2% in the optimal case compared to Case 2 in year 1, year 5, and year 10, respectively.

Fig. 12 presents the total imported active power to the substation from the upstream network in each season in year 1, year

TABLE IX
VOLTAGE AMPLITUDE AT BUSES 16, 17, 18, 31, 32, AND 33 AT THE PEAK LOAD HOUR FOR A TYPICAL SUMMER DAY IN YEAR 1, YEAR 5, AND YEAR 10 (P.U.)

		Bus Number					
		16	17	18	31	32	33
Case 1	Year 1	0.936	0.935	0.935	0.938	0.938	0.937
	Year 5	0.916	0.915	0.915	0.917	0.916	0.916
	Year 10	0.906	0.906	0.905	0.903	0.903	0.903
		Bus Number					
		16	17	18	31	32	33
Case 2	Year 1	0.935	0.934	0.934	0.936	0.935	0.934
	Year 5	0.914	0.913	0.913	0.911	0.910	0.909
	Year 10	0.903	0.903	0.902	0.902	0.901	0.901

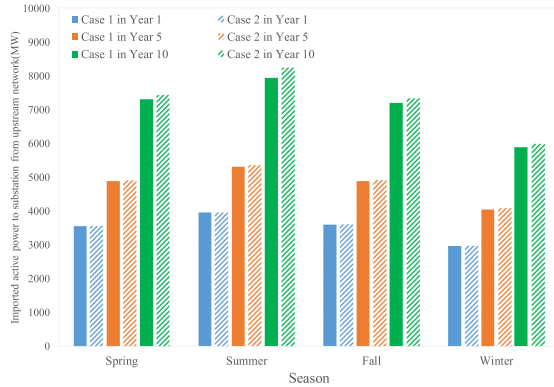


Fig. 12. Total imported active power to the substation from the upstream network in different seasons in year 1, year 5, and year 10.

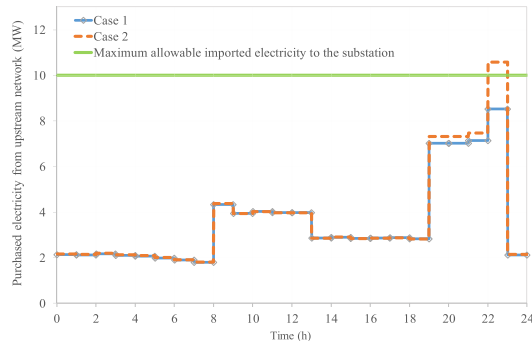


Fig. 13. Purchased electricity from upstream network for a typical summer day in year 10.

5, and year 10. It can be seen that the imported energy from the upstream network in Case 1 is always less than that in Case 2. For example, the total imported active power to the substation in the summer season in Case 1 is 8.53, 42.77, and 297.14-MW less than that in Case 2 in year 1, year 5, and year 10 in the same condition, respectively. Moreover, by annual comparison of results, it is shown that the imported electrical power in Case 1 is 36.23, 128.96, and 658.45 MW less than that in Case 2 in year 1, year 5, and year 10, respectively. Thus, the results verify the importance of μ EH placement in the IENGDS, especially for the final year. Therefore, the purchased energy is reduced in Case 1 during the planning horizon compared to Case 2.

Fig. 13 shows the purchased electricity from the upstream network for a typical day in summer in year 10. Moreover, Table X shows purchased electricity from the upstream network for a typical day in different seasons and different years at hours

TABLE X
PURCHASED ELECTRICITY FROM THE UPSTREAM NETWORK AT HOURS 20 AND 23 FOR A TYPICAL DAY IN DIFFERENT SEASONS IN YEAR 1, YEAR 5, AND YEAR 10 (MW)

		t=20			t=23		
		Year 1	Year 5	Year 10	Year 1	Year 5	Year 10
Case 1	Spring	2.699	3.607	5.654	1.08	1.667	2.384
	Summer	3.361	4.549	7.02	3.75	5.413	8.532
	Fall	2.712	3.36	5.553	1.282	1.769	2.394
	Winter	2.105	2.787	4.073	1.186	1.75	2.495
Case 2	Spring	2.699	3.61	5.828	1.086	1.694	2.442
	Summer	3.366	4.577	7.311	3.813	5.746	10.588
	Fall	2.712	3.603	5.676	1.299	1.806	2.455
	Winter	2.105	2.787	4.09	1.196	1.783	2.566

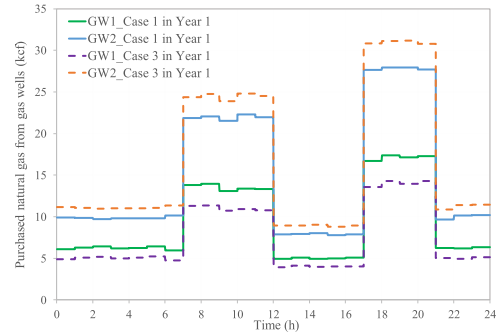


Fig. 14. Imported natural gas from two gas wells (GW1 and GW2) for a typical winter day in year 1.

20 and 23. It is shown, that the purchased electricity in Case 2 is always more than that in Case 1. According to Table X, especially in the summer season during the peak load hours, i.e., hours 20–23, and high tariff hours, i.e., hours 19–22, purchased electricity in Case 1 is less than that in Case 2 in the same condition. Thus, Case 1 could reduce operation costs during the planning horizon compared to the Case 2. In addition, according to Fig. 13, the imported electricity in Case 2 at some hours may exceed the maximum allowable limit, such as hour 23. This additional imported energy in Case 2 can potentially cause line congestion and affect the thermal rating constraints of the lines, especially in hot months.

Besides the electrical distribution network, the optimal locations of μ EHs could also improve the operation of the natural gas system. Fig. 14 compares the imported natural gas from gas wells in Case 1 (optimal case) and Case 3, during a typical winter day in year 1. Please note that the Case 2 has the same natural gas node connections (i.e., same imported natural gas) as Case 1. It should be mentioned that according to the results, imported natural gas from gas well 1 in Case 1 is more than that in Case 3, because μ EHs are connected closer to the gas well 1 in the Case 1 compared to the Case 3. However, according to the assumptions, gas well 2 has more capacity compared to gas well 1. Thus, Case 1 receives less natural gas from two gas wells compared to Case 3. For example, according to Fig. 14, it can be seen that the total received natural gas from gas wells during the selected winter day in Case 1 is 0.7-kcf less than that in Case 3.

Fig. 15 shows the imported natural gas from gas well 2 in node 8 in different seasons in year 1, year 5, and year 10. The imported natural gas from the selected gas well in the winter season is reduced by 9.75%, 10.64%, and 11.11% in Case 1 compared to

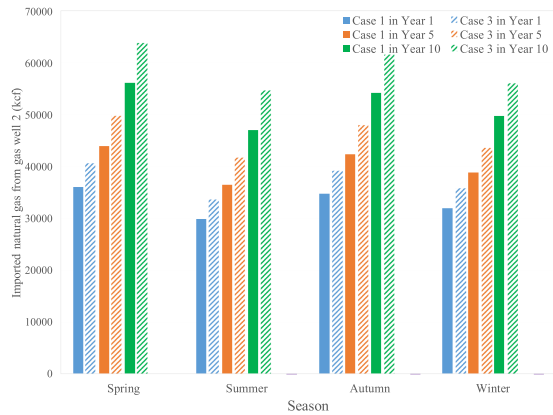


Fig. 15. Imported natural gas from gas well 2 at node 8 in different seasons in year 1, year 5, and year 10.

TABLE XI
GAS FLOW THROUGH THE PIPELINES FOR A TYPICAL WINTER DAY AT PEAK LOAD HOUR IN DIFFERENT YEARS (KCF)

	Case 1	Case 3
Year 1	192.917	205.764
Year 2	202.564	216.112
Year 3	212.694	226.99
Year 4	223.413	238.533
Year 5	234.898	251.006
Year 6	247.544	265.006
Year 7	261.13	280.173
Year 8	274.762	295.711
Year 9	288.476	310.721
Year 10	305.877	332.312

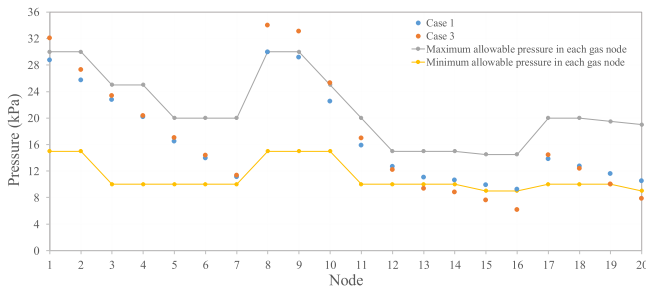


Fig. 16. Node gas pressure at a peak load hour of a typical winter day in year 10.

Case 2 in year 1, year 5, and year 10, respectively. Moreover, the results show that the total purchased natural gas from two gas wells in Case 1 is 269, 349, and 483-kcf less than those in Case 3 in year 1, year 5, and year 10, respectively. Moreover, Table XI presents total gas flow through the pipelines for a typical winter day at peak load hour (i.e., hour 20) in different years. Results show that the total gas flow through the pipelines in Case 1 is 6.2%, 6.4%, and 8% less than those in Case 3 in year 1, year 5, and year 10, respectively. Therefore, the operation cost and condition of the proposed natural gas system have been improved in the optimal case by decreasing the purchased natural gas.

Fig. 16 shows the profile of the gas pressure for a typical winter day at the peak hour (i.e., hour 20) in year 10. It is observed that in Case 3, the excessive pressure drop occurs at nodes 13, 14, 15, 16, and 20 at the peak load hour. Moreover, in Case 3, overpressure happens at nodes 1, 8, 9, and 10 at the peak load hour. As a result, in year 10 of Case 3, the gas flow

through the pipeline 8–9 exceeds its intended capacity of 50 kcf. Accordingly, in Case 1, the natural gas system operates in an optimal and feasible condition, i.e., the pressures of gas nodes are between the minimum and maximum allowable pressure of each node, during the whole planning horizon.

It is worth noting that there are marginal gaps for variables in NLP and MINLP problems. If values of marginal gaps are close to zero, then optimal conditions are provided in the problem. Simulation results show that marginal gaps of variables in both steps are close to zero. Therefore, computational efficiency is acceptable. Moreover, according to [47], the BONMIN solver can guarantee global optimal solutions for the proposed planning model in the IENGDS.

IV. CONCLUSION

This article presented a hierarchical planning model to design the optimal capacity of μ EHs components and the optimal locations of μ EHs in an IENGDS. The impacts of seasonal climate changes on energy demands and prices were considered during the planning horizon, and the uncertainties in demands and renewable energy generation were quantified and managed with a two-stage stochastic programming framework.

The effectiveness of the planning model was evaluated on an IENGDS that consists of an IEEE 33-bus distribution system and a Belgian 20-node natural gas system, with three difference scenarios. The results showed that in the optimal case: 1) The total line losses at a peak load hour could be reduced by up to 27.5%; 2) the total purchased electricity from the upstream network could be reduced by up to 3.5%; 3) the total imported natural gas from gas wells could be reduced by 103 kcf in winter days; 4) the IENGDS could operate in an optimal condition without potential electricity network congestion or natural gas pressure violations during the planning horizon. Therefore, the optimal case in the hierarchical planning problem shows that the performance of IENGDS such as line losses, energy usage, and cost can be improved compared to other cases during the planning horizon. Because in the other cases, the μ EHs are installed only with the opinion of the μ EH operators, and concerns of the IENGDS operator are not considered. As future works, more interaction between μ EHs and IENGDS for selling surplus energy of μ EHs to the distribution system, reconfiguration of IENGDS, and reliability indices in the objective function of the IENGDS planning-step could be considered in the problem.

REFERENCES

- [1] M. Geidl and G. Andersson, "Optimal power flow of multiple energy carriers," *IEEE Trans. Power Syst.*, vol. 22, no. 1, pp. 145–155, Feb. 2007.
- [2] H. Sadeghi, M. Rashidinejad, M. Moeini-Aghtaie, and A. Abdollahi, "The energy hub: An extensive survey on the state of the art," *Appl. Thermal Eng.*, vol. 161, 2019, Art. no. 114071.
- [3] M. Geidl, G. Koeppl, P. Favre-Perrod, B. Klockl, G. Andersson, and K. Frohlich, "Energy hubs for the future," *IEEE Power Energy Mag.*, vol. 5, no. 1, pp. 24–30, 2006.
- [4] M. Geidl, "Integrated modeling and optimization of multi-carrier energy systems," Ph.D. dissertation, Swiss Fed. Inst. Technol., ETH, Zurich, Switzerland, 2007.
- [5] D. Rakipour and H. Barati, "Probabilistic optimization in operation of energy hub with participation of renewable energy resources and demand response," *Energy*, vol. 173, pp. 384–399, 2019.

- [6] A. Dolatabadi and B. Mohammadi-Ivatloo, "Stochastic risk-constrained scheduling of smart energy hub in the presence of wind power and demand response," *Appl. Thermal Eng.*, vol. 123, pp. 40–49, 2017.
- [7] L. Bai, F. Li, H. Cui, T. Jiang, H. Sun, and J. Zhu, "Interval optimization based operating strategy for gas-electricity integrated energy systems considering demand response and wind uncertainty," *Appl. Energy*, vol. 167, pp. 270–279, 2016.
- [8] C. Shao, Y. Ding, P. Siano, and Y. Song, "Optimal scheduling of the integrated electricity and natural gas systems considering the integrated demand response of energy hubs," *IEEE Syst. J.*, vol. 15, no. 3, pp. 4545–4553, Sep. 2021.
- [9] L. Bhamidi and S. Sivasubramani, "Optimal planning and operational strategy of a residential microgrid with demand side management," *IEEE Syst. J.*, vol. 14, no. 2, pp. 2624–2632, Jun. 2020.
- [10] G. Mavromatidis, K. Orehounig, and J. Carmeliet, "Design of distributed energy systems under uncertainty: A two-stage stochastic programming approach," *Appl. Energy*, vol. 222, pp. 932–950, 2018.
- [11] R. Jing *et al.*, "A multi-objective optimization and multi-criteria evaluation integrated framework for distributed energy system optimal planning," *Energy Convers. Manage.*, vol. 166, pp. 445–462, 2018.
- [12] B. Mohammadi-Ivatloo and F. Jabari, *Operation, Planning, and Analysis of Energy Storage Systems in Smart Energy Hubs*. Cham, Switzerland: Springer, 2018.
- [13] S. Senemar, M. Rastegar, M. Dabbaghjamanesh, and N. D. Hatzigiorgiou, "Dynamic structural sizing of residential energy hubs," *IEEE Trans. Sustain. Energy*, vol. 11, no. 3, pp. 1236–1246, Jul. 2020.
- [14] A. Dolatabadi, B. Mohammadi-Ivatloo, M. Abapour, and S. Tohidi, "Optimal stochastic design of wind integrated energy hub," *IEEE Trans. Ind. Informat.*, vol. 13, no. 5, pp. 2379–2388, Oct. 2017.
- [15] Y. Wang *et al.*, "Research on capacity planning and optimization of regional integrated energy system based on hybrid energy storage system," *Appl. Thermal Eng.*, vol. 180, 2020, Art. no. 115834.
- [16] M. Karmellos and G. Mavrotas, "Multi-objective optimization and comparison framework for the design of distributed energy systems," *Energy Convers. Manage.*, vol. 180, pp. 473–495, 2019.
- [17] Z. Luo *et al.*, "Multi-objective capacity optimization of a distributed energy system considering economy, environment and energy," *Energy Convers. Manage.*, vol. 200, 2019, Art. no. 112081.
- [18] Y. Wang, N. Zhang, Z. Zhuo, C. Kang, and D. Kirschen, "Mixed-integer linear programming-based optimal configuration planning for energy hub: Starting from scratch," *Appl. Energy*, vol. 210, pp. 1141–1150, 2018.
- [19] S. A. Mansouri, A. Ahmarinejad, M. S. Javadi, and J. P. Catalão, "Two-stage stochastic framework for energy hubs planning considering demand response programs," *Energy*, vol. 206, 2020, Art. no. 118124.
- [20] M. A. Mirzaei, M. Nazari-Heris, B. Mohammadi-Ivatloo, K. Zare, M. Marzband, and A. Anvari-Moghaddam, "A novel hybrid framework for co-optimization of power and natural gas networks integrated with emerging technologies," *IEEE Syst. J.*, vol. 14, no. 3, pp. 3598–3608, Sep. 2020.
- [21] G. T. Ayele, M. T. Mabrouk, P. Haurant, B. Laumert, and B. Lacarrière, "Optimal placement and sizing of heat pumps and heat only boilers in a coupled electricity and heating networks," *Energy*, vol. 182, pp. 122–134, 2019.
- [22] C. Qin, Q. Yan, and G. He, "Integrated energy systems planning with electricity, heat and gas using particle swarm optimization," *Energy*, vol. 188, 2019, Art. no. 116044.
- [23] H. Wang, C. Gu, X. Zhang, and F. Li, "Optimal CHP planning in integrated energy systems considering network charges," *IEEE Syst. J.*, vol. 14, no. 2, pp. 2684–2693, Jun. 2020.
- [24] S. Pazouki, A. Mohsenzadeh, S. Ardalan, and M.-R. Haghifam, "Optimal place, size, and operation of combined heat and power in multi carrier energy networks considering network reliability, power loss, and voltage profile," *IET Gener., Transmiss. Distrib.*, vol. 10, no. 7, pp. 1615–1621, 2016.
- [25] S. Xie, Z. Hu, J. Wang, and Y. Chen, "The optimal planning of smart multi-energy systems incorporating transportation, natural gas and active distribution networks," *Appl. Energy*, vol. 269, 2020, Art. no. 115006.
- [26] A. Naderipour, Z. Abdul-Malek, S. A. Nowdeh, V. K. Ramachandaramurthy, A. Kalam, and J. M. Guerrero, "Optimal allocation for combined heat and power system with respect to maximum allowable capacity for reduced losses and improved voltage profile and reliability of microgrids considering loading condition," *Energy*, vol. 196, 2020, Art. no. 117124.
- [27] B. Arandian and M. Ardehali, "Renewable photovoltaic-thermal combined heat and power allocation optimization in radial and meshed integrated heat and electricity distribution networks with storages based on newly developed hybrid shuffled frog leaping algorithm," *J. Renewable Sustain. Energy*, vol. 9, no. 3, 2017, Art. no. 033503.
- [28] G. Li, R. Zhang, T. Jiang, H. Chen, L. Bai, and X. Li, "Security-constrained bi-level economic dispatch model for integrated natural gas and electricity systems considering wind power and power-to-gas process," *Appl. Energy*, vol. 194, pp. 696–704, 2017.
- [29] C. Wu, W. Gu, Y. Xu, P. Jiang, S. Lu, and B. Zhao, "Bi-level optimization model for integrated energy system considering the thermal comfort of heat customers," *Appl. Energy*, vol. 232, pp. 607–616, 2018.
- [30] Y. Li, Z. Li, F. Wen, and M. Shahidehpour, "Privacy-preserving optimal dispatch for an integrated power distribution and natural gas system in networked energy hubs," *IEEE Trans. Sustain. Energy*, vol. 10, no. 4, pp. 2028–2038, Oct. 2019.
- [31] A. Mirzapour-Kamanaj, M. Majidi, K. Zare, and R. Kazemzadeh, "Optimal strategic coordination of distribution networks and interconnected energy hubs: A linear multi-follower bi-level optimization model," *Int. J. Elect. Power Energy Syst.*, vol. 119, 2020, Art. no. 105925.
- [32] H. Xiao, W. Pei, Z. Dong, and L. Kong, "Bi-level planning for integrated energy systems incorporating demand response and energy storage under uncertain environments using novel metamodel," *CSEE J. Power Energy Syst.*, vol. 4, no. 2, pp. 155–167, 2018.
- [33] S. Senemar, A. R. Seifi, M. Rastegar, and M. Parvania, "Probabilistic optimal dynamic planning of onsite solar generation for residential energy hubs," *IEEE Syst. J.*, vol. 14, no. 1, pp. 832–841, Mar. 2020.
- [34] M. Salimi, H. Ghasemi, M. Adelpour, and S. Vaez-Zadeh, "Optimal planning of energy hubs in interconnected energy systems: A case study for natural gas and electricity," *IET Gener., Transmiss. Distrib.*, vol. 9, no. 8, pp. 695–707, 2015.
- [35] A. Alabdulwahab, A. Abusorrah, X. Zhang, and M. Shahidehpour, "Stochastic security-constrained scheduling of coordinated electricity and natural gas infrastructures," *IEEE Syst. J.*, vol. 11, no. 3, pp. 1674–1683, Sep. 2017.
- [36] M. Aien, M. G. Khajeh, M. Rashidinejad, and M. Fotuhi-Firuzabad, "Probabilistic power flow of correlated hybrid wind-photovoltaic power systems," *IET Renewable Power Gener.*, vol. 8, no. 6, pp. 649–658, 2014.
- [37] Z. Zhou, J. Zhang, P. Liu, Z. Li, M. C. Georgiadis, and E. N. Pistikopoulos, "A two-stage stochastic programming model for the optimal design of distributed energy systems," *Appl. Energy*, vol. 103, pp. 135–144, 2013.
- [38] S. Pazouki and M.-R. Haghifam, "Optimal planning and scheduling of energy hub in presence of wind, storage and demand response under uncertainty," *Int. J. Elect. Power Energy Syst.*, vol. 80, pp. 219–239, 2016.
- [39] T. Ding, Y. Hu, and Z. Bie, "Multi-stage stochastic programming with nonanticipativity constraints for expansion of combined power and natural gas systems," *IEEE Trans. Power Syst.*, vol. 33, no. 1, pp. 317–328, Jan. 2018.
- [40] C. Sahin, M. Shahidehpour, and I. Erkmen, "Allocation of hourly reserve versus demand response for security-constrained scheduling of stochastic wind energy," *IEEE Trans. Sustain. Energy*, vol. 4, no. 1, pp. 219–228, Jan. 2013.
- [41] M. Majidi and K. Zare, "Integration of smart energy hubs in distribution networks under uncertainties and demand response concept," *IEEE Trans. Power Syst.*, vol. 34, no. 1, pp. 566–574, Jan. 2019.
- [42] California Energy Commission, *Assessment of California CHP Market and Policy Options for Increased Penetration*. Sacramento, CA, USA: California Energy Commission, 2005.
- [43] S. Steam, "Industrial combustion boilers," *Combustion/Industrial Testing*, pp. 1–5, May 2010.
- [44] H. Ibrahim and A. Ilinca, "Techno-economic analysis of different energy storage technologies," in *Energy Storage-Technologies and Applications*. London, U.K.: IntechOpen, 2013.
- [45] M. G. Gulaliyev, E. R. Mustafayev, and G. Y. Mehdiyeva, "Assessment of solar energy potential and its ecological-economic efficiency: Azerbaijan case," *Sustainability*, vol. 12, no. 3, 2020, Art. no. 1116.
- [46] Y. Cheng and C. Zhang, "Configuration and operation combined optimization for EV battery swapping station considering PV consumption bundling," *Protection Control Modern Power Syst.*, vol. 2, no. 1, pp. 1–18, 2017.
- [47] M. R. Bussieck and S. Vigerske, "MINLP solver software," in *Wiley Encyclopedia of Operations Research and Management Science*. Hoboken, NJ, USA: Wiley, 2010.